Pergamon

0148-9062(95)00058-5

Int. J. Rock Mech. Min. Sci. & Geomech. Abstr. Vol. 33, No. 2, pp. 111–123, 1996

0148-9062/96 $15.00 + 0.00

A Hierarchical Model of Rough Rock Joints Based on Micromechanics

J.-J. DONG†
Y.-W. PAN†‡

A rough rock joint model is proposed in this study on the basis of micromechanics concepts. In the model, the global behavior of a rough joint depends on the microfeatures of the contact planes on the joint. The contact mechanics on contact planes controls the mechanical behavior of the joint via a homogenization process. Also, the complex mechanical behavior of a joint is associated with simple microfeatures of the joint, including the frictional properties and the structure of contact planes. To capture the feature of scale dependency of joint roughness, a hierarchical representation of a joint profile is proposed in the form of a multi-level-asperity model. Moreover, the constitutive relation of the multi-level-asperity model is derived through a recursive homogenization process. The proposed model's framework is general and systematic. Furthermore, major deformation mechanisms of joint asperities, i.e. interlocking, wearing, shearing-off, sliding, separation and degradation, are taken into account.

1. INTRODUCTION

Many mechanical models describe joint behavior, of which, phenomenological models based on plasticity theory comprise the majority [1–6]. Phenomenological models, however, have several disadvantages in modeling joint behavior. First, the required parameters in these models lack any physical meaning because plasticity-theory treats joints as a continuum. Besides, a phenomenological approach of a joint model cannot explicitly take into account the contact mechanisms under loading. Accordingly, a structural approach seems preferable in modeling joints since contact mechanisms predominate the mechanical behavior of a joint.

A rough rock joint's mechanical behavior under loading involves the interaction of irregular joint surfaces. The micro-contact effects on these surfaces determine the macroscopic response of the joint. On the basis of the contact theory of two rough surfaces [7,8], Swan [9] directly correlated the normal stiffness with the topography of joint wall. In his work, the global joint behavior was evaluated via the joint roughness profiling technique by measuring joint height variation. Later, Swan and Zongqi [10] extended this work to consider the shear behavior of joints. The extended model was later verified by Sun *et al.* [11]. These models assume the occurrence of elastic contact and do not explicitly consider asperity degradation. For practical use, the statistical profiling data of natural joint surfaces must be analyzed [12,13]. This procedure appears time-consuming and inefficient.

Alternatively, following the "$\phi + i$" concept [14], the joint topography is often modeled as a set of regular asperities in most structural approaches. Ladanyi and Archambault [15], in their pioneering work, proposed a widely used joint strength model originated from granular mechanics [16–18]. They considered riding up or shearing through the asperity as two major mechanisms controlling the global behavior of joints. On the basis of this concept, Amadei and Saeb [19] proposed a constitutive model of a rock joint based on the modified theory of Ladanyi and Archambault [20]. Their model takes into account the coupling shear behavior of a joint resulting from dilatancy and the boundary effect. Theoretically taking the irregularity of the joint surface into account is really impossible. One alternative, then, is to use certain empirical indexes and make a correlation [21,22]. The well-known JRC–JCS models [23–29] represent this branch of "$\phi + i$" approaches. Considering the geometry of joint surface and the relative degraded strength, this category of simple models correlates two empirical variables (JRC and JCS) with the joint behavior observed. As a result, the mechanism of joints under compression and shear is captured to a certain extent.

By modeling joint behavior as an interaction problem between two media, Plesha [30] later developed a

†Institute of Civil Engineering, National Chiao-Tung University, Hsinchu 30050, Taiwan, R. O. China.
‡To whom all correspondence should be addressed.

macroscopic constitutive law of joints through microstructural consideration. The joint surface is idealized as a triangular saw-tooth model and the yield function is linked to micro level sliding criterion of contact area. This plasticity-based joint model illustrates the mechanism of joint behavior through means of microscopic features. The model captures well the sliding mechanism along contact surface well. Moreover, this model incorporates a wear theory to account for the degradation of joint asperities under cyclic loading. The model has been further extended to model the joint asperities in a sinusoidal shape [31,32]. Through a local slip criterion in the contact level, the model bridges the big gap between the phenomenological and structural model of rock joints. On the basis of the same concept, Jing [33] modeled the softening behavior of a joint using hardening and softening functions.

Recently, Haberfield and Johnston [34] reviewed the limitations of available joint models and proposed a mechanistically-based joint model. In their investigation, by using joint roughness and a few basic rock properties as model parameters, the capability of the structural model was demonstrated through simulating shear behavior of joints under constant normal stiffness (CNS) condition. Their model treats a joint profile as a series of irregular triangular asperities capable of sustaining elastic deformation. The asperities can also be sheared off if the shear stress on the joint exceeds a certain limit. In their model, the distribution of normal stress on each asperity must be determined. As stated by Haberfield and Johnston [34], using a complex numerical procedure to determine the normal stress distribution of each asperity is impractical. Instead, they proposed a simplified but approximate alternative that involves several assumptions. However, this procedure makes the solution somewhat indirect.

In this study, a conceptual model is proposed by considering the microscopic contact features of rough rock joints. The successful application of micromechanics to granular materials [35] has led toward modeling the rock joint behavior in this approach. This model is a micromechanics based homogenization process controlled by a friction law and contact plane orientation. A multi-level roughness model represents the statistical nature of a joint surface. Therefore, the scale dependent property of joint roughness can be simulated in a relatively easy approach via the hierarchical roughness representation. In this model, any level of asperity can be smoothed if the stress state exceeds certain critical conditions. As a result, this model can simulate the effects of interlocking and degradation of micro-asperities. The softening behavior of a joint can also be modeled by the gradual change in the orientation of contact planes (degrading from an initial inclined angle to a certain residual value). The global behavior of a joint can be determined easily from the micro-feature of the basic contact plane on which the frictional law and degradation law applies. The number of required parameters in this model are relatively few; in addition, each material parameter processes a physical meaning. The proposed model's framework is more straightforward than other conventional models. Moreover, the contact interaction can be solved more directly using this approach than the simplified approach adopted by Haberfield and Johnston.

2. THE BASICS OF THE MICROMECHANICS-BASED MODEL

2.1. Fundamental concepts of micromechanics-based joint model

A micromechanics-based model is presented in this work to describe the mechanical behavior of a rock joint. The following concepts are fundamental elements in the proposed model.

2.1.1. Basic contact plane. A rock joint is considered as two rough rock surfaces in contact with each other. The characteristics of contact rock surfaces control the global mechanical behavior of a joint. To simplify the complicated contact mechanics, a real contact point is represented by a smooth basic contact plane using the homogenization concept. On this plane, the Amonton's friction law is assumed here to apply. Selecting basic contact planes depends on the stress level and the joint scale. Small undulation (thereby resulting in the interlocking effect [36,37]) on joint faces tends to become smoothened quickly after shearing action. Unless the mechanical behavior of a joint under very low magnitude of shear stress is concerned, one need not select a very small basic contact plane to model the contact problem in a rock joint.

2.1.2. Hierarchical contact structure. An actual joint-face frequently undulates irregularly. Uniform orientation distribution of contact planes may oversimplify the nature of a real joint. Different approaches are proposed to represent the actual joint surface geometry. Roberts *et al.* [38] proposed a systematic framework capable of describing the joint surface geometry in either a deterministic approach, statistical approach, or probabilistic approach. Alternatively, fractal geometry [39] was used to model a joint surface by treating the joint surface as a self-similar surface [40,41]. This fractal geometry approach seems promising. To account for the scale dependence of joint roughness, the representation of joint surface as a self-affine surfaces appears more reasonable [42–44]. In addition, joint roughness can be represented in any desired resolution using the self-affine fractal. Following a similar concept, the proposed model considers the contact structure within a rock joint as a multi-level hierarchical system. The asperity of a rock joint is represented as multi-level asperities in a saw-tooth shape, as illustrated in Fig. 1. The orientation of saw teeth can be random in any level. The basic contact planes are composed of the outward boundary of the lowest level asperity (which is also in a saw-tooth shape). On the basis of micro-mechanistic formulation, the contact behavior of asperity along basic contact planes (which is the lowest level asperity) can determine the mechanical behavior of the higher level asperities through a homogenization process. The global (average)

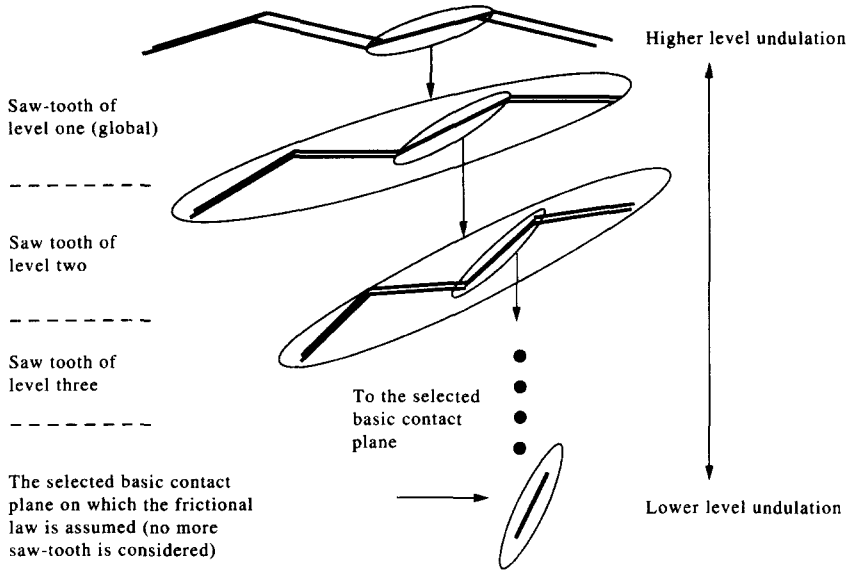

Fig. 1. The hierarchical structure of joint profile.

mechanical behavior of a joint can thus be obtained in a recursive procedure. The single saw-tooth shape surface represents a special case in which only one level of asperity is considered.

2.1.3. Deformation mechanism. Johnston and Lam [36] observed several basic mechanisms controlling joint movement. These basis mechanisms include: (i) initial deformation; (ii) asperity sliding (including the smoothening of micro-asperities which subsequently causes sudden loss of the apparent cohesion); (iii) asperity shearing; and (iv) asperity crushing. To simplify the complex process of joint deformation, three dominant mechanisms influencing joint deformation are considered in the proposed model, i.e.: (i) the elastic contact deformation (in the initial deformation stage); (ii) the relative sliding of contact plane (in the asperity sliding stage); and (iii) the degradation of joint wall which may include the smoothening of the relative micro asperities, the wearing effect, and the crushing (damaging) of the macro asperity. In developing the proposed model, the following assumptions are made concerning the micromechanistic deformation mechanism on a basic contact plane: (i) The contact materials deform elastically before the shearing stress on a basic contact plane reaches the frictional strength on the plane. The frictional strength on the contact plane is determined from the basic frictional angle, (ii) Sliding between the contact rock materials occurs when the shear stress reaches the frictional strength on the contact plane. Consequently, the shear stress on the contact plane becomes equal to the frictional strength during sliding, (iii) If the average shear stress on a micro saw tooth of any level exceeds the joint-wall strength, degradation of the saw tooth occurs simultaneously and the basic contact plane gradually changes in the degradation process, (iv) The complicated nature of degradation of a macro saw tooth (which may include tensile cracks in the saw tooth and the wearing on the contact plane) can be simplified by a degradation process. A gradual degradation process can model the effect of wearing on the contact plane; on the other hand, a rapid degradation process may model brittle behavior due to the tensile breakage of a saw tooth.

2.2. The proposed model's framework

Micromechanics has been successfully applied in recent years to model the mechanical behavior of granular materials [35,45]. In a micromechanical model, the macro behaviors of granular assemblage are a function of the microstructure and micro properties of particles. Following a similar concept, the proposed model obtains a macrofeature from micro feature through a homogenization process. The process is based on the following basic relations:

(1) between the local contact stress and the average stress,
(2) between the local relative displacement and the average relative displacement,
(3) between the local contact stress and the local relative displacement (i.e. the local constitutive law).

It is assumed that the local constitutive law of the basic contact plane is elastic before yielding. After yielding, the sliding and separation effects of contact plane can be considered through a relaxation stress [35]. The averaged stress and relative displacement is derived through a homogenization process, as shown in Fig. 2. The micromechanics-based constitutive model of a rock joint is derived in an incremental form.

3. SINGLE-LEVEL-ASPERITY CONSTITUTIVE MODEL OF JOINT

3.1. Model formulation

Figure 3 illustrates the coordinate system and the stress components used in the following formulation. The stress components, σ_N^g and σ_S^g, are the global normal stress and shear stress, respectively, on the global joint plane (i.e. the average joint plane). The stress tensors, σ_n^c and σ_s^c, are the local contact normal stress and shear

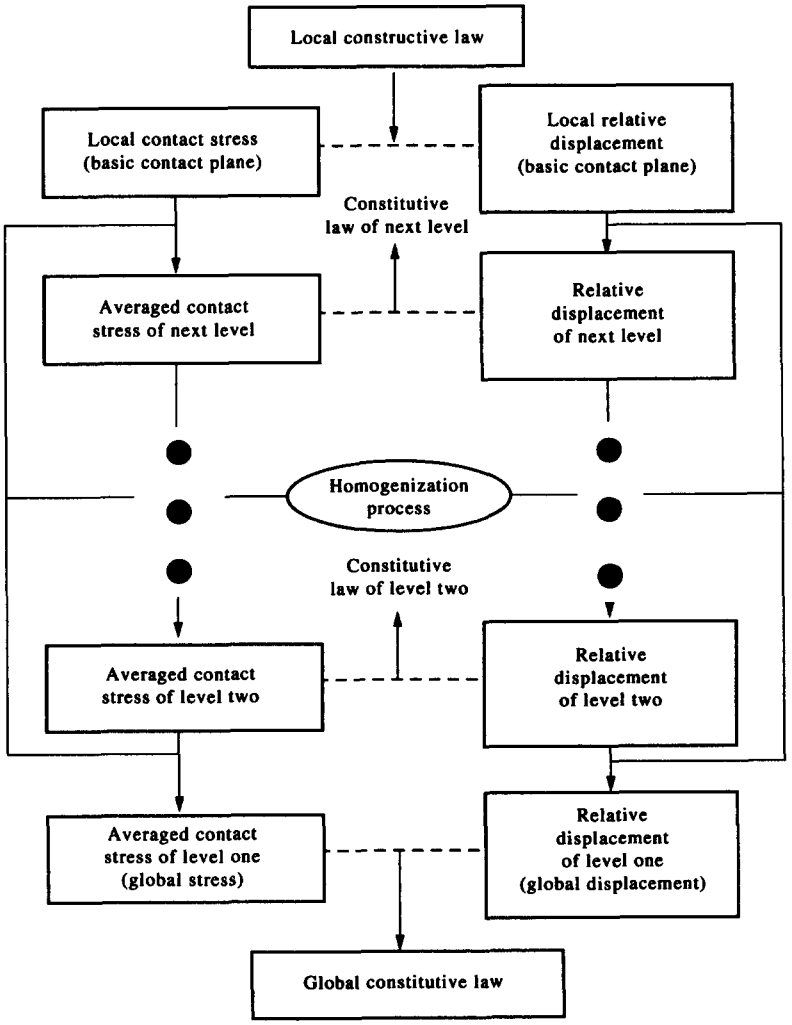

Fig. 2. Framework of the proposed model.

stress, respectively, on the local contact plane (i.e. the basic contact plane).

From the equilibrium conditions, the increment of global stress tensor, $d\sigma_i^g$, can be obtained by first transforming the local contact stresses tensor, $d\sigma_i^c$, into the global coordinates system then summing up their total. Hence,

$$d\sigma_i^g = \frac{1}{A_0}\sum_{c=1}^{N} a^c T_{ij}^c d\sigma_j^c, \tag{1}$$

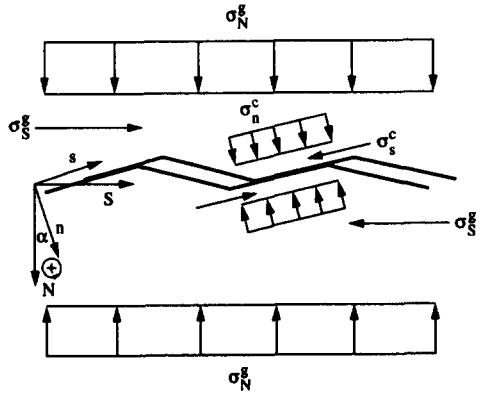

Fig. 3. The coordinate system of the single level model.

where

A_0 is the global cross-sectional area of joint,
a^c is the selected contact area of the basic contact plane "c",
T_{ij}^c is a coordinate transformation tensor (from the local coordinate system to the global coordinate system) depending on the orientation of the contact plane. For the plane strain condition: $T_{nn} = T_{ss} = \cos\alpha$, $T_{ns} = -T_{sn} = \sin\alpha$, in which α is the inclined angle of the contact plane, as shown in Fig. 3,
N is the total number of selected basic contact planes.

The local constitutive law of the basic contact plane regulates the relation between the local contact stresses tensor, $d\sigma_i^c$, and the local relative displacement tensor, du_j^c, of the basic contact plane "c". This constitutive law can be expressed as

$$d\sigma_i^c = k_{ij}^c du_j^c - dr_i^c, \tag{2}$$

in which k_{ij}^c is the contact stiffness tensor of the basic contact plane "c", and dr_i^c is the relaxation stress tensor that accounts for the sliding and separation effects on the contact plane. When sliding occurs, the shear component of the relaxation stress is taken as the amount of contact shear stress exceeding the contact shear strength.

When separation occurs, the normal component of the relaxation stress is taken as the amount of the contact normal stress exceeding the contact tensile strength. The tensile strength is zero if no adhesive material in the joint is present.

Inserting equation (2) into equation (1) yields

$$d\sigma_i^g = \frac{1}{A_0}\sum_{c=1}^{N} a^c T_{ij}^c k_{jk}^c du_k^c - \frac{1}{A_0}\sum_{c=1}^{N} a^c T_{ij}^c dr_j^c. \quad (3)$$

The global relative displacement, du_j^g, can also be obtained by averaging the local relative displacements, du_j^c, according to

$$du_i^g = \sum_{c=1}^{N} T_{ij}^c du_j^c. \quad (4)$$

A heterogeneous tensor H^c is next introduced to account for the variational nature of the local relative displacement. Correspondingly, the local relative displacement is derived as

$$du_i^c = T_{ij}^{c-1} H_{kj}^c du_j^g. \quad (5)$$

The heterogeneous tensor, H_{kj}^c, accounts for the variation of local relative displacement, du_j^c. If the local relative displacement is uniformly distributed over a contact plane, an identity tensor represents the heterogeneous tensor. Otherwise, a suitable statistical distribution should be considered in modeling the non-uniform distribution of the local relative displacement over a contact plane.

Inserting equation (5) into equation (3), yields the following expression.

$$d\sigma_i^g = \frac{1}{A_0}\sum_{c=1}^{N} a^c T_{ij}^c k_{jk}^c T_{kl}^{c-1} H_{lm}^c du_m^g - \frac{1}{A_0}\sum_{c=1}^{N} a^c T_{ij}^c dr_j^c \quad (6a)$$

or

$$d\sigma_i^g = K_{ij} du_j^g - dR_i, \quad (6b)$$

where K_{ij} and dR_i are the global stiffness and relaxation stress tensor, respectively. K_{ij} is a function of the contact plane orientation and local contact stiffness. The relaxation stress tensor, dR_i, reflects the local yielding condition.

3.2. *Verification*

Numerical simulation of a symmetrical saw-tooth shaped joint is presented in this subsection to demonstrate the validity of the proposed model. Each saw tooth contains a pair of contact planes with a positive slope and negative slope, respectively, to form a triangular asperity. For simplicity, additional assumptions (besides the fundamental assumptions) are made in the numerical simulations (although these assumptions are not essential in the proposed model).

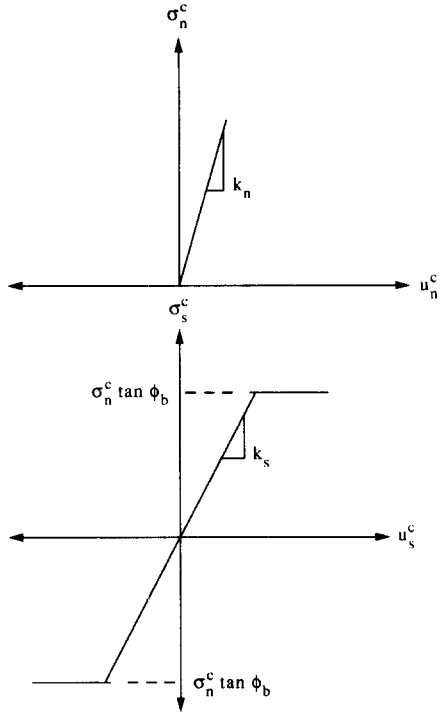

Fig. 4. The local constitutive law of the basic contact plane.

(1) Contact bodies deform linear-elastically before relative sliding or separation occurs. (Figure 4 illustrates the local constitutive law.)
(2) The contact shear stress on the contact plane does not exceed the sliding shear strength, τ_f, as defined by the friction law $\tau_f = \sigma_n \tan \phi_b$. In which σ_n and ϕ_b are the normal stress and the basic frictional angle, respectively.
(3) Plane-strain condition is considered.
(4) The bodies on two sides of the joint are initially matched perfectly.
(5) The local relative displacement is identical to the global relative displacement through coordinate transformation. Hence, the heterogeneous tensor becomes an identity tensor.

To verify the proposed model, a comparison is made of model simulation results with the experimental data of artificial regular joints of saw-tooth shape [32]. Table 1 lists the parameters used in the simulation. The single-level-asperity model is capable of accurately depicting a saw-tooth shaped joint. Hence, this model can successfully capture the shear behavior of joint with a relatively simple calculation. Figure 5 shows the compressive deformation and the shear dilation of the experimental data. Results of the model simulation are shown in Fig. 6.

Through a proper correlation of asperity inclination with accumulated shear displacement, the proposed

Table 1. Parameters selected for verifying the presented micromechanics based model

Basic friction angle	Inclined angle of asperity	Normal stiffness	Shear stiffness
$\phi_b = 39.8°$	$\alpha = 10°$	$k_n = 15$ MPa/mm	$k_s = 13$ MPa/mm

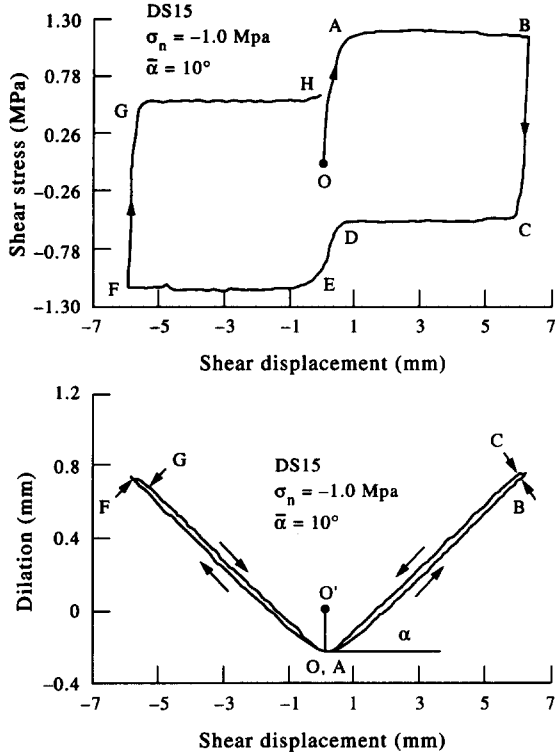

Fig. 5. Experimental data of artificial joints (retrieved from [32]).

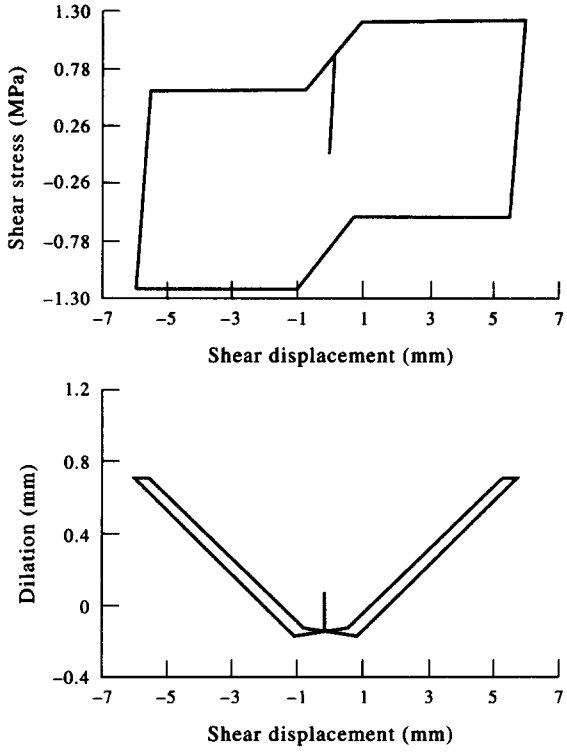

Fig. 6. Simulated results of artificial regular joints by single-level model.

model can be expanded easily to simulate the wearing effect of asperity under cyclic shearing. Such an example is the wear theory adopted by Plesha and co-workers [30,31]. This subject is not covered in detail here. Figures 7 and 8 present the simulation results of cyclic shearing, in which the wear effect is taken into account.

3.3. *Discussion*

The proposed single-level-asperity model has been verified in the above by making a comparison of simulation and experimental results for an artificial saw-tooth joint. Unsurprisingly, simulation results are quite close

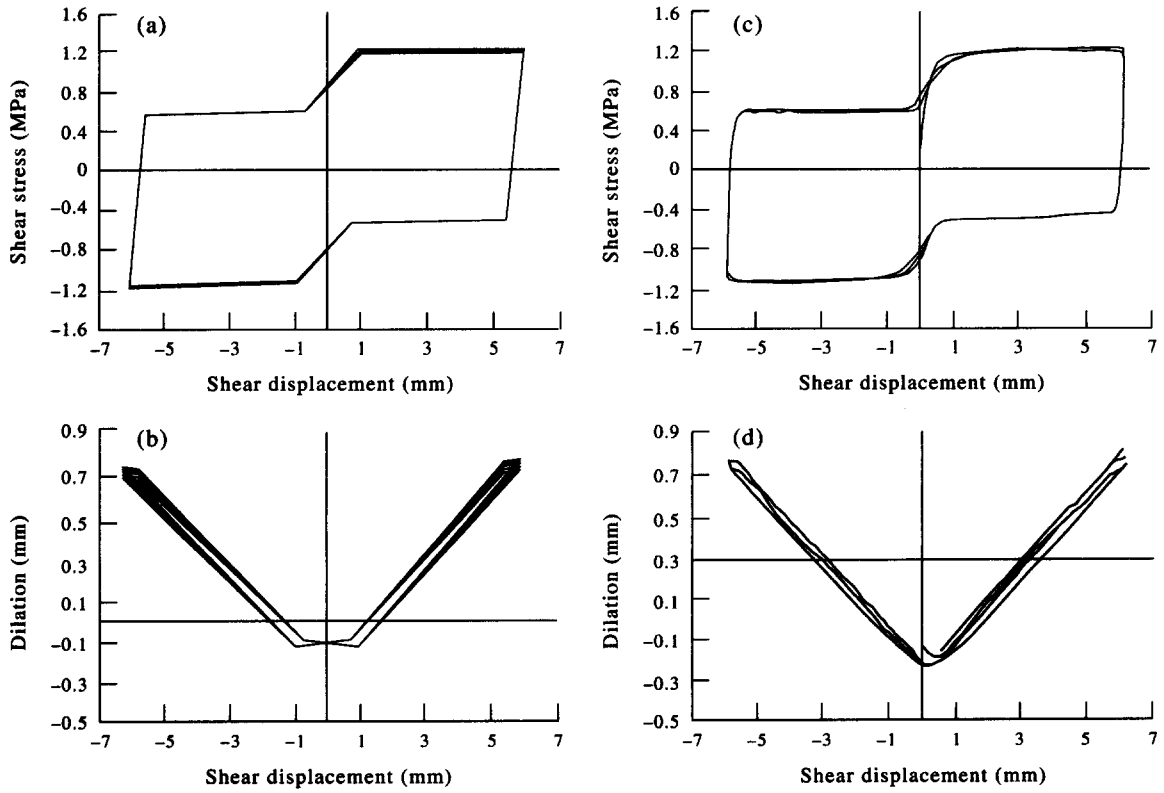

Fig. 7. (a) and (b) Simulated results for the first five cycles of a direct shear test; (c) and (d) experimental results (normal stress = 1.0 MPa) (retrieved from [31]).

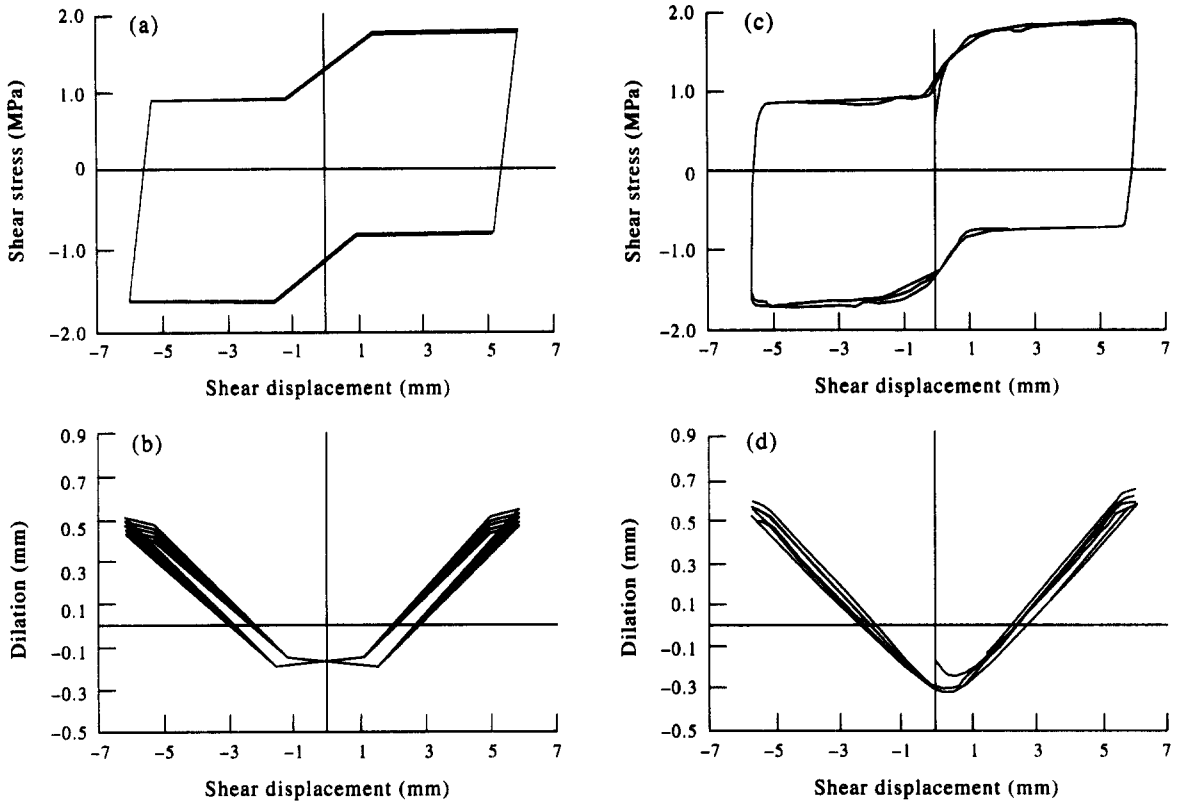

Fig. 8. (a) and (b) Simulated results for the second five cycles of a direct shear test; (c) and (d) experimental results (normal stress = 1.5 MPa) (retrieved from [31]).

to those of Plesha's model [32] since the deformation mechanisms considered in both models are similar (in spite of the differences in the formulation of two models). The proposed model, however, makes use of only four basic parameters to capture the shear and compressive behavior of a regular joint. Consequently, the required calibration effort can be significantly reduced. A detailed calibration procedure and a parametric study are presented in Section 5. The amount of calculation required in the model simulation is relatively light.

The single-level-asperity model just presented generally follows the "$\phi + i$" concept, in which the angle "i" represents the inclined angle of joint asperity. However, natural joints are frequently irregular, and natural joint roughness is very different from an ideal saw-tooth model. Joint roughness generally has a random and scale-dependent nature. In a practical measurement, joint roughness depends primarily on the relative scale of selected base length for measuring the joint roughness. Micro-roughness on a joint controls the mechanical behavior of the joint only when the stress level and relative scale are relatively small. As the stress level or scale increases, the importance of micro-roughness' role degrades rapidly. Micro-asperities can become smoothened quickly once the shear stress is sufficiently large. Absolutely defining the inclined angle of joint asperity is relatively difficult since joint roughness is a scale-dependent parameter. With this aspect in mind, a hierarchical concept of joint roughness is next proposed to expand the single-level-asperity model into a so-called "multi-level-asperity model". The formulation and simulation of the multi-level-asperity model are presented in the subsequent sections.

4. MULTI-LEVEL-ASPERITY CONSTITUTIVE MODEL OF JOINT

4.1. Model formulation

The homogenized (average) mechanical behavior of level one asperity determines the global mechanical behavior of a joint, as shown in Fig. 1. Let $d({}^1\sigma_i^g)$ and $d({}^1u_j^g)$ denote the incremental global averaged stress tensor and the global averaged relative displacement tensor, respectively. The left headnote number denotes the averaged level of asperity homogenized, and the right headnote specifies the particular contact plane homogenized. For instance, $d({}^1\sigma_i^g)$ is the incremental average stress on the global (average) plane of the joint (in level-one asperity). By using a similar formulation as presented in the last section, the generalized global constitutive law can be formulated as follows.

$$d({}^1\sigma_i^g) = {}^1K_{ij}^g d({}^1u_j^g) - d({}^1R_i^g). \tag{7}$$

The tensor ${}^1K_{ij}^g$ is the global averaged stiffness and can be expressed by

$${}^1K_{ij}^g = \frac{1}{{}^1A_0}\sum_{n=1}^{{}^1N^g} {}^2A^n\,{}^2T_{ik}^n\,{}^2K_{kl}^n\,({}^2T_{lm}^n)^{-1}\,{}^2H_{mj}^n, \tag{8}$$

in which ${}^2K_{kl}^n$ is the local stiffness tensor of the nth contact plane in the level-two averaged (asperity) plane, and ${}^1N^g$ is the total number of averaged contact planes in level-one asperity.

$d({}^1R_i^g)$ is the global relaxation stress tensor expressed by

$$d({}^1R_i^g) = \frac{1}{{}^1A_0} \sum_{n=1}^{{}^1N^g} {}^2A^n \, {}^2T_{ij}^n \, d({}^2R_j^n). \tag{9}$$

${}^1K_{ij}^g$ is a function of the averaged contact plane orientation and the averaged contact stiffness ${}^2K_{kl}^n$ in level-two asperity homogenized.

Following the same line of homogenization process, every averaged contact stiffness in the level-two asperity is a function of the contact plane orientation and averaged contact stiffness in the level-three asperity. Therefore,

$${}^2K_{ij}^n = \frac{1}{{}^2A^n} \sum_{s=1}^{{}^2N^n} {}^3A^s \, {}^3T_{ik}^s \, {}^3K_{kl}^s ({}^3T_{lm}^s)^{-1} \, {}^3H_{mj}^s, \tag{10}$$

$$d({}^2R_i^n) = \frac{1}{{}^2A^n} \sum_{s=1}^{{}^2N^n} {}^3A^s \, {}^3T_{ij}^s \, d({}^3R_j^s), \tag{11}$$

in which ${}^3K_{kl}^s$ is the local stiffness tensor of the sth contact plane in the level-three averaged (asperity) plane, ${}^2N^n$ is the total number of averaged contact planes in level-two asperity of nth averaged plane, and $d({}^3R_i^g)$ is the relaxation stress tensor in the level-three averaged (asperity) plane.

The recursive process can proceed until the level of a basic contact plane (e.g. the pth level) is reached. The averaged stiffness, ${}^{p-1}K_{ij}^c$, and the relaxation tensors, $d({}^{p-1}R_i^c)$, in the level $(p-1)$ averaged (asperity) plane can be expressed as follows:

$${}^{p-1}K_{ij}^c = \frac{1}{{}^{p-1}A^c} \sum_{b=1}^{{}^{p-1}N^c} {}^pA^b \, {}^pT_{ik}^b \, k_{kl}^b ({}^pT_{lm}^b)^{-1} \, {}^pH_{mj}^b, \tag{12}$$

$$d({}^{p-1}R_i^c) = \frac{1}{{}^{p-1}A^c} \sum_{b=1}^{{}^{p-1}N^c} {}^pA^b \, {}^pT_{ij}^b \, d(r_j^b), \tag{13}$$

in which k_{kl}^b and $d(r_j^b)$ denote the basic contact stiffness and relaxation tensor, respectively, of the contact plane "b". These two tensors depend on the deformation mechanisms, as previously described in Section 3. In the above equation, ${}^{p-1}N^c$ is the total number of basic contact planes in level $(p-1)$ asperity of the cth averaged plane.

Micro-roughness tends to be smoothened (shearing-off) when the stress state reaches a certain critical condition. To model this aspect, a low level asperity is allowed to disappear when the average shear stress in that level exceeds a shear strength τ_s (which obeys $\tau_s = \sigma_n \tan \phi_s$ in which σ_n is the normal stress and ϕ_s is the shearing-off angle). The shearing-off of the micro asperities only starts from the asperities of the lowest level and may proceed to the asperities of a higher level if the shear stress rises any further.

Following the recursive formulation described above, the global stiffness ${}^1K_{ij}^g$ and the global relaxation stress tensor $d({}^1R_i^g)$ can be derived from the local constitutive relations on the basic contact plane (i.e. the lowest level asperity) through homogenization as shown in Fig. 2.

4.2. Demonstration

A comparison of the simulated and laboratory direct shear tests of slate joint [10] is made in Fig. 9 to

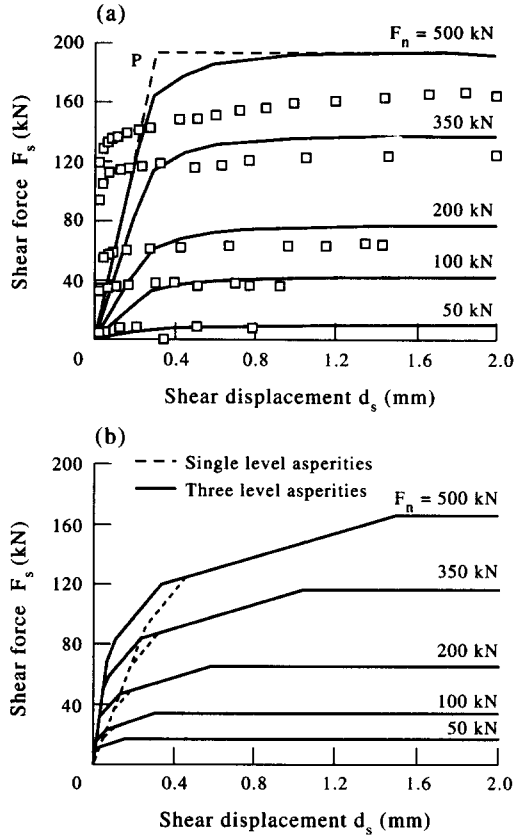

Fig. 9. (a) Laboratory and simulated direct shear test of slate joint (retrieved from [10]). (□ experimental result—simulation by Barton–Bandis model.) (b) Simulated direct shear test of slate joint by the proposed model.

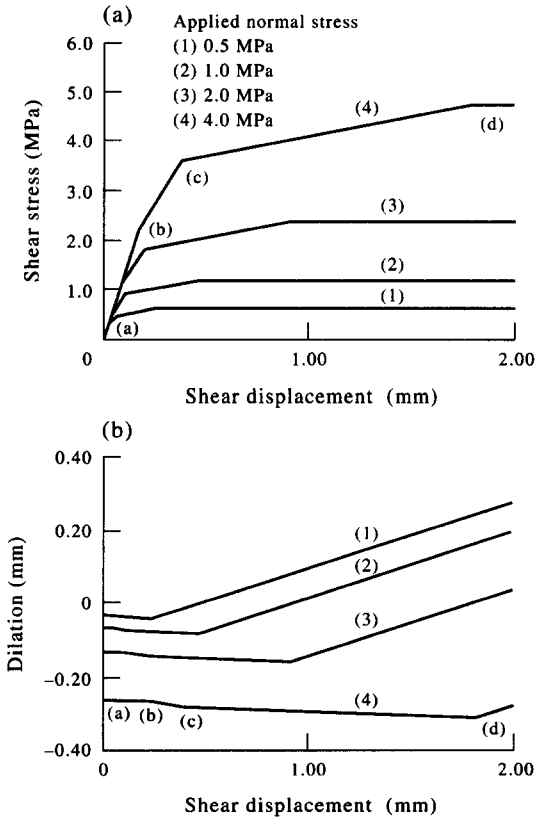

Fig. 10. The influence of normal stress on the shear behavior of a regular joint under direct shear. (a) Shear stress vs shear displacement; (b) dilation vs shear displacement.

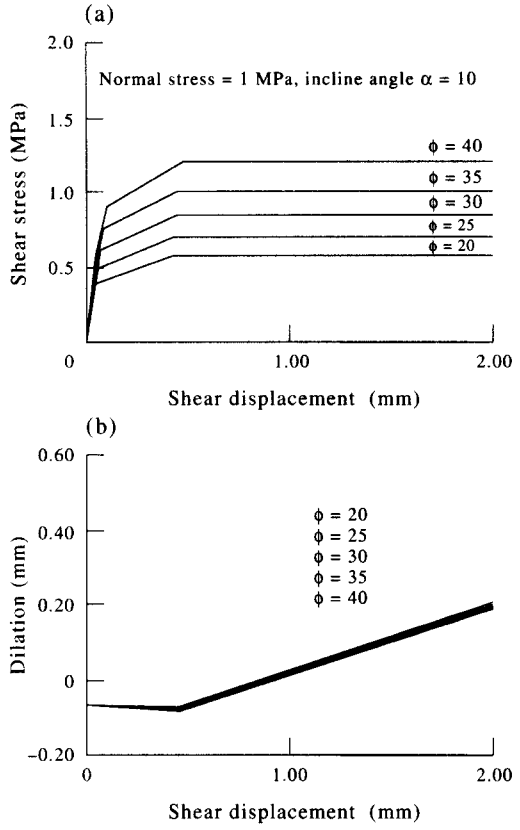

Fig. 11. The influence of basic friction angle on the shear behavior of a regular joint under direct shear: (a) shear stress vs shear displacement; (b) dilation vs shear displacement.

demonstrate the validity of the multi-level model. The assumptions stated in Section 3.2 are still preserved in this part. Joint models with single and three level(s), respectively, of triangular saw-tooth asperity are considered. The parameters used in the simulation are: (1) the basic friction angle $\phi_b = 12°$; (2) the inclined angle of the 1st level asperity = 6.21°, inclined angle of the 2nd and 3rd level asperity = 26.21°; and (3) the normal stiffness $k_n = 50$ MPa/mm and the shear stiffness $k_s = 5$ MPa/mm. The frictional and inclined angle of the 1st level asperity are adopted from [10]. The other parameters are selected arbitrarily. The simulation results correlate sufficiently with the experimental results. A substantial improvement in the accurate prediction of initial stiffness of nature joints over the simulation results by other $\phi + i$'s model [dashed line of Fig. 9(a)] can be observed.

As Fig. 9(b) shows, the selected levels of asperities affect the initial shear stiffness of the joint model. Adopting higher levels of asperities not only implies an increase in the relative roughness implicitly, but also represents a greater number of micro-contacts sharing the external loads. Interlocking of these micro-contacts can largely constrain the mobility of relative shear displacement of a joint. Any model treating a joint surface only as an averaged saw-tooth shape can never capture this phenomenon thoroughly. Figure 9(b) also reveals that the ultimate strength is independent of the levels of asperities considered because the selected shear-off strength of the relative micro-level asperities is small ($\phi_s = 10°$ in both 2nd and 3rd levels). In practice, micro-asperities tend to smoothen under a small shear displacement as long as the shear stress becomes quite large relative to the strength of joint wall. As a result, most interlocking micro-contacts vanish eventually and the macro-asperity controls the ultimate behavior of the joint. This accounts for why those models adopting $\phi + i$'s concept can only predict ultimate behavior, but fail to accurately describe the initial stage of a loaded joint.

5. PARAMETERS CALIBRATION AND PARAMETRIC STUDY

5.1. Determination of the parameters

The proposed model uses only a few parameters, i.e. basic frictional angle and local stiffness. A method to obtain these parameters is described in this subsection. The basic friction angle and the local stiffness (of a contact plane) can be determined by compressive and shearing tests on two smooth surfaces. The basic frictional angle of a common rock type can be easily found in previous literature involving the mechanical properties of rock materials [46]. Available information regarding the local stiffness is not as common as those of basic frictional angle. However, we will demonstrate later that the local stiffness of contact plane plays an insignificant role, particularly when the ultimate shear strength is the major concern.

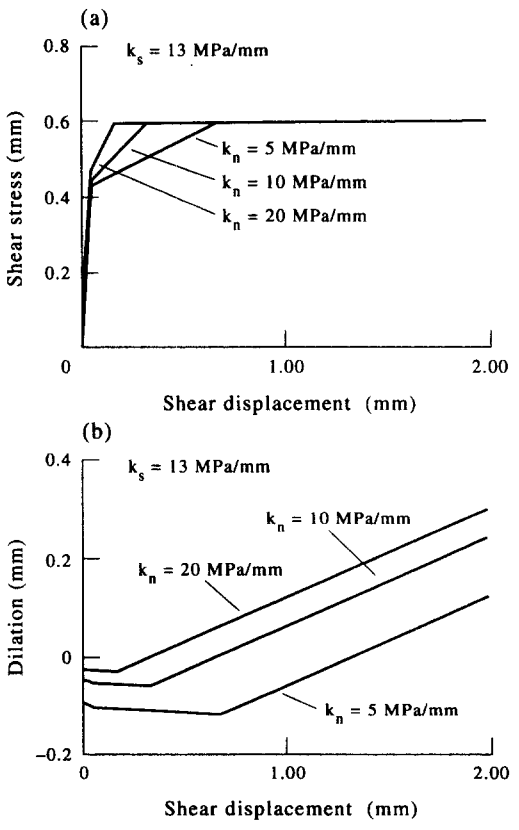

Fig. 12. The influence of local normal stiffness on the shear behavior of a regular joint under direct shear: (a) shear stress vs shear displacement; (b) dilation vs shear displacement.

5.2. Parametric study

A parametric study is next presented to investigate the influences of single level joint asperity microfeatures on the direct shear behavior of a joint under a constant normal loading condition (Figs 10–15). The parametric study in this section makes use of the same assumptions as in Section 3.2 to represent the microfeatures of joint asperity. For simplicity, regular saw-tooth shaped asperity without degradation is assumed unless noted otherwise. The parameters used (if not presented in the figures) can be found in Table 1. The normal stress σ_n is 0.5 MPa in the simulations presented in Figs 12 and 13 and 1.0 MPa in others unless noted otherwise.

The local constitutive law on a basic contact plane contains a sliding criterion and a local stiffness. The normal loading and the basic frictional angle are the dominant factors governing the sliding mechanism. Figure 10 reveals that the shear strength is proportional to the normal loading. Each curve in Fig. 10 can be divided into four segments: (1) segment *ab*-elastic deformation; (2) segment *bc*-relative sliding of the contact surface with negative slope; (3) segment *cd*-separation of the contact surface with negative slope; and (4) segment after *d*-relative sliding of the contact surface with positive slope. This figure also reveals that the shear displacement corresponding to the onset of the 4th segment (relative sliding along all contact surfaces) increases with an increase in normal loading. The increase in normal loading subsequently reduces joint dilation, but does not affect the dilation rate after the occurrence of relative

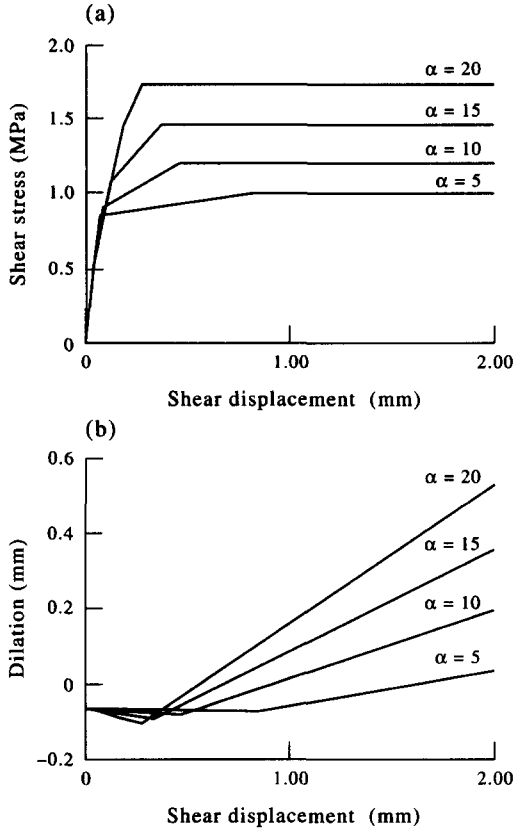

Fig. 14. The influence of inclined angle on the shear behavior of a regular joint under direct shear: (a) shear stress vs shear displacement; (b) dilation vs shear displacement.

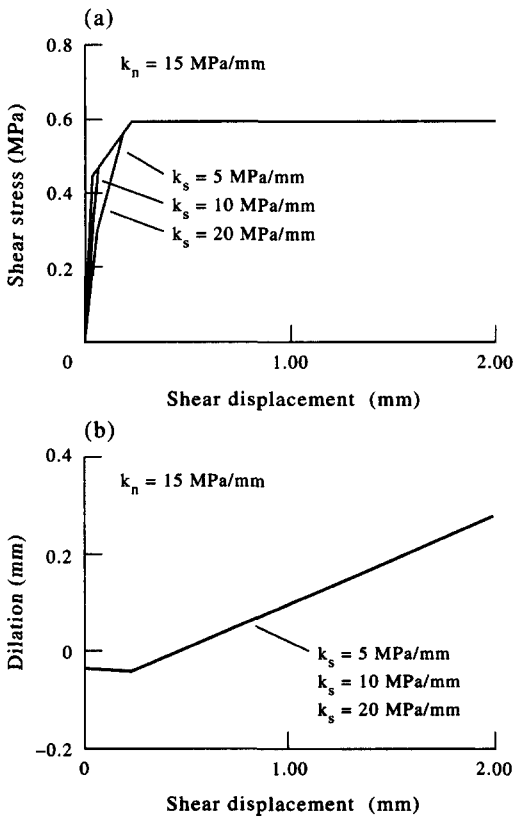

Fig. 13. The influence of local shear stiffness on the shear behavior of a regular joint under direct shear: (a) shear stress vs shear displacement; (b) dilation vs shear displacement.

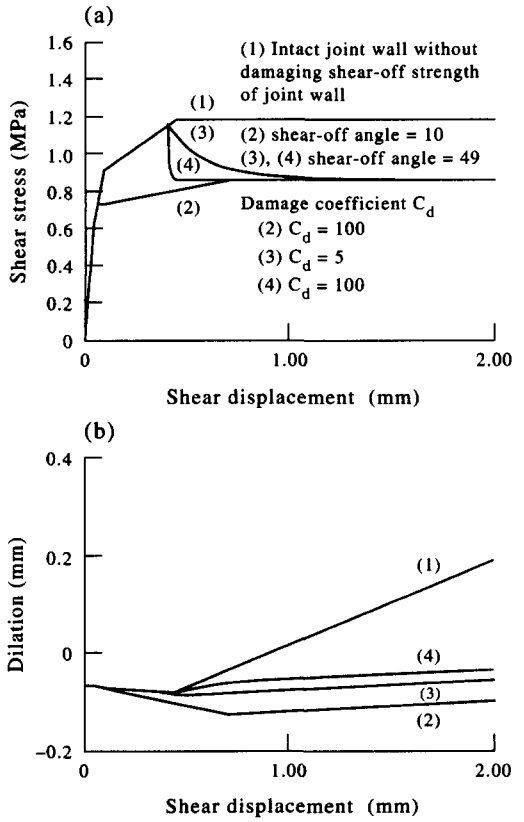

Fig. 15. The influence of joint wall strength on the shear behavior of a regular joint under direct shear: (a) shear stress vs shear displacement; (b) dilation vs shear displacement.

sliding. The dilation rate only depends on the orientation of the contact plane. The basic frictional angle is a fundamental parameter of frictional materials. Figure 11 reveals that: (i) the shear strength of joint increases with the basic frictional angle; (ii) the basic frictional angle affects neither dilation nor dilation rate; and (iii) the basic frictional angle does not affect the initial slope of the curve of shear stress versus shear deformation.

Figures 12 and 13 present the influences of local stiffness on joint deformation. Figure 12(a) shows that: (i) local normal stiffness does not significantly affect the initial stiffness and shear strength of a joint; (ii) the normal deformation under compression and the shear displacement after yielding increase with a decrease in the local normal stiffness, k_n. Figure 12(b) shows that the dilation rate remains constant. The influence of local shear stiffness is presented in Fig. 13. Local shear stiffness affects the initial curve of shear stress vs shear deformation, but does not alter the shear strength and dilation curve.

Figure 14 shows that the shear strength of a joint increases with the inclined angle of the contact plane. The dilation rate after yielding is exactly equal to the inclined angle of the contact plane. The orientation of contact plane plays a role similar to the dilation angle of granular materials. This role reflects the influence of joint roughness to the shear behavior of the joint.

The joint asperities may be crushed or gradually worn down to a residual shape under stress. The degradation process may further derive from the development of tensile cracks within the joint wall [47]. The actual mode of degradation depends on the stress field within the joint wall. However, this stress field is highly complicated; in addition, analytically modeling this aspect is impractical. Alternatively, the combined degradation or damaging process can be modeled by a degradation law which considers a continuous change in the orientation of a contact plane from an initial state to a residual one. In an averaging concept, the onset of degradation can be assumed to occur when the averaged shear stress reaches a certain limit (which can be regarded as an equivalent shear strength of joint wall). Next, a hypothetical degradation law is proposed herein for demonstration purposes. The contact inclined angle α is assumed to be a function of the accumulated plastic work w_p as follows.

$$\alpha = \alpha_r + (\alpha_0 - \alpha_r)e^{-c_d \cdot w_p} \tag{14}$$

in which α_0 is the initial contact inclined angle before any degradation occurs; α_r is the residual contact inclined angle after the degradation process is complete; c_d is degradation coefficient which reflects the speed of asperity degradation.

Figure 15 presents the effect of joint-asperity degradation under various joint wall strengths. Curve 1 in this figure shows the simulation results without joint-asperity degradation. The ultimate strength can be obtained by combining the inclined angle without degradation ($\alpha_0 = 10°$) and the basic frictional angle ($\phi_b = 39.8°$). If the averaged shear stress on joint wall exceeds the joint-wall strength, the joint tooth starts degrading (curves 2–4). The hardening or softening behavior depends on the strength and degradation process of the joint-wall. When the joint-wall strength is relatively high (e.g. curves 3 and 4, $\phi_s = 49°$), the curve shows a softening behavior from the peak to a residual strength. The residual contact inclined angle is set to be 1° in cases 2–4. The only difference between curves 3 and 4 is the selected degradation coefficient c_d (5 and 100, respectively) which reflects the speed of degradation. The softening behavior will not exist if the joint-wall strength is relatively low (as shown in curve 2, $\phi_s = 10°$). Furthermore, for cases 2–4, the dilation rates after yielding are all equal to the residual inclined angle.

The proposed model can simulate the mechanical behavior of rock joint under a variety of conditions. The proposed model, which is derived in an incremental form, can take the stress-path effect into account without much difficulty. Besides, model simulation can take the effects of boundary and system-stiffness conditions into account. Figure 16 demonstrates the capability of the proposed model to simulate the shear behavior of joint under CNL (constant normal loading) and CNS (constant normal stiffness) conditions. The system stiffness is assigned infinity to simulate the boundary condition of a constrained normal dilation. Figure 16(a) indicates that the joint stiffness under constrained normal displacement condition arises after a large shear displacement develops. Because the joint dilatancy [dashed line in Fig. 16(b)] is constrained, the normal loading tends to increase. This effect also increases the ultimate strength

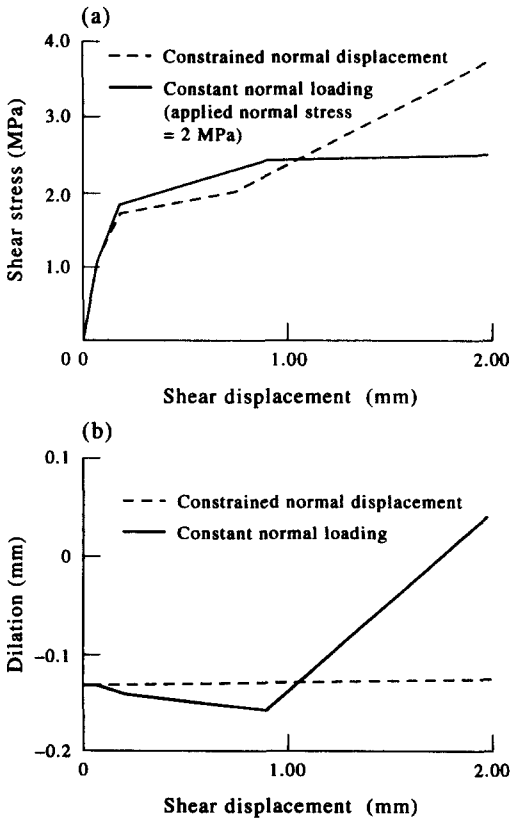

Fig. 16. The influence of boundary condition on the shear behavior of a regular joint under direct shear: (a) shear stress vs shear displacement; (b) dilation vs shear displacement.

of the joint. Under this condition, the degradation mechanism of asperity may control the shear behavior of the joint.

6. SUMMARY AND CONCLUSIONS

A model of rough rock joints based on micromechanics concepts has been proposed in this study. In the proposed model, the global behavior of a rough joint depends upon the microfeatures of the contact planes on the joint. Through a homogenization process, the contact mechanics on contact planes control the mechanical behavior of the joint. Thus, the complex mechanical behavior of a joint is linked with simple microfeature of the joint, including the frictional properties and the structure of contact planes. To capture the feature of scale dependency of joint roughness, a hierarchical representation of joint profile has been proposed in a form of multi-level-asperity model. Moreover, the constitutive relation of the multi-level-asperity model is derived through a recursive process of homogenization.

The proposed model's framework is general and systematic. Major deformation mechanisms, i.e. including sliding and separation between contact planes, interlocking and shearing-off effects of micro roughness, wearing and degradation of joint tooth on joint asperity, are taken into account. The global constitutive law is derived in an incremental form. Hence, the proposed model can take the stress dependency of joint behavior into account without much difficulty. This model requires only a few parameters which can be either calibrated or estimated easily. The numerical implementation of this model is quite simple. Accordingly, it can be easily incorporated with a common numerical tool to simulate the mechanical behavior of rock masses.

Accepted for publication 18 May 1995.

REFERENCES

1. Ghaboussi J., Wilson E. L. and Isenberg J. Finite element for rock joints and interfaces. *J. Soil Mech. Found. Div. ASCE* **99,** 833–848 (1973).
2. Roberts W. J. and Einstein H. H. Comprehensive model for rock discontinuities. *J. Geotech. Engng* **104,** 553–569 (1978).
3. Heuze F. E. and Barbour T. G. New models for rock joints and interfaces. *J. Geotech. Engng* **108,** 757–776 (1982).
4. Desai C. S. and Fishman K. L. Constitutive model for rocks and discontinuities (joints). *Proc. 28th Symp. Rock Mech.*, Tucson, Arizona (1987).
5. Desai C. S. and Fishman K. L. Plasticity-based constitutive model with associated testing for joints. *Int. J. Rock Mech. Min. Sci. & Geomech. Abstr.* **28,** 15–26 (1991).
6. Desai C. S. and Ma Y. Modelling of joints and interfaces using the disturbed-state concept. *Int. J. Numerical Analytical Methods Geomech.* **16,** 623–653 (1992).
7. Greenwood J. A. and Tripp J. H. The contact of two nominally flat rough surfaces. *Proc. Inst. Mech. Engrs* **185,** 625–633 (1971).
8. Johnson K. L. *Contact Mechanics.* Cambridge Univ. Press, London (1985).
9. Swan G. Determination of stiffness and other joint properties from roughness measurement. *Rock Mech. Rock Engng* **16,** 19–38 (1983).
10. Swan G. and Zongqi S. Prediction of shear behaviour of joints using profiles. *Rock Mech. Rock Engng* **18,** 183–212 (1985).
11. Sun Z., Gerrard C. and Stephansson O. Rock joint compliance tests for compression and shear loads. *Int. J. Rock Mech. Min. Sci. & Geomech. Abstr.* **22,** 197–213 (1985).
12. Wu T. H. and Ali E. M. Statistical representation of joint roughness. *Int. J. Rock Mech. Min. Sci. & Geomech. Abstr.* **15,** 259–336 (1987).
13. Krahn J. and Morgenstern N. R. The ultimate frictional resistance of rock discontinuities. *Int. J. Rock Mech. Min. Sci. & Geomech. Abstr.* **16,** 127–133 (1979).
14. Patton F. D. Multiple modes of shear failure in rock and related materials. Ph.D. thesis, Univ. of Illinois (1966).
15. Ladanyi B. and Archambault G. Simulation of shear behavior of a jointed rock mass. *Proc. 11th Symp. Rock Mech., AIME*, New York, pp. 105–125 (1970).
16. Newland P. L. and Allely B. H. Volume changes in drained triaxial tests on granular materials. *Geotechnique* **7,** 17–34 (1957).
17. Rowe P. W. The stress-dilatancy relation for static equilibrium of an assembly of particles in contact. *Proc. R. Soc. Lond.* **269,** 500–527 (1962).
18. Rowe P. W., Barden I. and Lee I. K. Energy components during the triaxial cell and direct shear tests. *Geotechnique* **14,** 247–267 (1964).
19. Amadei B. and Saeb S. Constitutive models of rock joints. *Proc. Int. Con. Rock Joints*, Loen, Norway, pp. 581–594 (1990).
20. Saeb S. A variance on the Ladanyi and Archambault's failure criterion. *Proc. Int. Con. Rock Joints*, Loen, Norway, pp. 701–705 (1990).
21. Tse T. and Cruden D. M. Estimating joint roughness coefficients. *Int. J. Rock Mech. Min. Sci. Geomech. Abstr.* **16,** 127–133 (1979).
22. Dight P. M. and Chiu H. K. Prediction of shear behaviour of joints using profiles. *Int. J. Rock Mech. Min. Sci. & Geomech. Abstr.* **18,** 369–386 (1981).
23. Barton N. A review of a new shear strength criterion for rock joints. *Engng Geol.* **7,** 287–332 (1973).
24. Barton N. Rock mechanics review, the shear strength of rock and rock joints. *Int. J. Rock Mech. Min. Sci. & Geomech. Abstr.* **13,** 255–279 (1976).
25. Barton N. and Choubey V. The shear strength of rock joints in theory and practice. *Rock Mech.* **10,** 1–54 (1977).
26. Bandis S. C., Lumsden A. C. and Barton N. Experimental studies of scale effects on the shear behavior of rock joints. *Int. J. Rock Mech. Min. Sci. & Geomech. Abstr.* **18,** 1–21 (1981).
27. Barton N. and Bandis S. C. Effects of block size on the shear behavior of jointed rock. *Proc. 23rd Symp. Rock Mech.*, Berkeley, Calif. (1982).
28. Bandis S. C., Lumsden A. C. and Barton N. Fundamentals of rock joint deformation. *Int. J. Rock Mech. Min. Sci. & Geomech. Abstr.* **20,** 249–268 (1983).
29. Bandis S., Barton N. and Bakhtar K. Strength, deformation and conductivity coupling of rock joints. *Int. J. Rock Mech. Min. Sci. & Geomech. Abstr.* **22,** 121–140 (1985).
30. Plesha M. E. Constitutive model for rock discontinuities with dilatancy and surface degradation. *International Journal for Numerical & Analytical Methods in Geomechanics* **11,** 345–362 (1987).
31. Qiu X.-J., Plesha M. E., Huang X. and Haimson B. C. An investigation of the mechanics of rock joints—Part II: analytical investigation. *Int. J. Rock Mech. Min. Sci. & Geomech. Abstr.* **30,** 313–321 (1993).
32. Huang X., Haimson B. C., Plesha M. E. and Qiu X.-J. An investigation of the mechanics of rock joints—Part I: laboratory investigation. *Int. J. Rock Mech. Min. Sci. & Geomech. Abstr.* **30,** 257–269 (1993).
33. Jing L. A two-dimensional constitutive model of rock joints with pre- and post-peak behaviour. *Proc. Int. Con. Rock Joints*, Loen, Norway, pp. 633–638 (1990).
34. Haberfield C. M. and Johnston I. W. A mechanistically-based model for rough rock joints. *Int. J. Rock Mech. Min. Sci. & Geomech. Abstr.* **31,** 279–292 (1994).
35. Chang C. S., Chang Y. and Kabir M. G. Micromechanics modelling for stress–strain behavior of granular soils I: theory. *J. Geotech. Engng* **118,** 1959–1974 (1992).
36. Johnston I. W. and Lam T. S. K. Shear behaviour of regular triangular concrete/rock joints-analysis. *J. Geotech. Engng Div. ASCE* **115,** 711–727 (1989).
37. Johnston I. W. and Lam T. S. K. Shear behaviour of regular triangular concrete/rock joints-evaluation. *J. Geotech. Engng Div. ASCE* **115,** 728–740 (1989).
38. Roberts W. J., Iwano M. and Einstein H. H. Probabilistic mapping of rock joint surfaces. *Proc. Int. Con. Rock Joints*, Loen, Norway, pp. 681–691 (1990).

39. Mandelbrot B. B. How long is the coast of Britain? Statistical self-similarity and the fractional dimension. *Science* **156,** pp. 636–638 (1967).
40. Turk N., Grieg M. J., Dearman W. R. and Amin F. F. Characterization of rock joint surfaces by fractal dimension. *Proc. 28th U.S. Symp. Rock Mech.*, Balkema. Boston, Mass., pp. 1223–1236 (1987).
41. Carr J. R. Fractal characterization of joint surface roughness in welded tuff of Yucca Mountain, Nevada. *Proc. 30th U.S. Symp. Rock Mech.*, Morgantown, West Virginia, pp. 193–200 (1989).
42. Mandelbrot B. B. Self-affine fractals and fractal dimension. *Physica Scripta* **32,** 257–260 (1985).
43. Huang S. L., Oelfke S. M. and Speck R. C. Applicability of fractal characterisation and modelling to rock joint profiles. *Int. J. Rock Mech. Min. Sci. & Geomech. Abstr.* **29,** 89–98 (1992).
44. Odling N. E. Natural fracture profiles, fractal dimension and joint roughness coefficients. *Rock Mech. Rock Engng* **27,** 135–153 (1994).
45. Mehrabadi M. M., Loret B. and Nemat-Nasser S. Incremental constitutive relations for granular materials based on micromechanics. *Proc. R. Soc. Lond. A* **441,** 433–463 (1993).
46. Lama R. D. and Vutukuri V. S. *Handbook on Mechanical Properties of Rocks*, Vol. 4. Trans Tech. Publications, Rockport, Mass. (1978).
47. Pereira J. P. and de Freitas M. H. Mechanisms of shear failure in artificial fractures of sandstone and their implication for models of hydromechanical coupling. *Rock Mech. Rock Engng* **26,** 195–214 (1993).